If the distortion were either tetragonal or trigonal, for example, the 3-fold degeneracy of the $|A\rangle$ state would be lifted and a pair of states of A_2 and E symmetries would result. The present results cannot distinguish between these two types of distortion in any easy way, but simple considerations in both cases lead to the prediction of a positive A term for the degenerate E state and B terms of opposite sign for the A_2 and E states, respectively, which would give rise to a positive pseudo A term if the two states are close in energy (within bandwidths). The combination of the A term for the E state and the pseudo A term for the interaction between the A_2 and E states would be expected to give an unsymmetrical MCD spectrum as observed. The A_2 state is likely lower in energy than the E state and has the negative B term because the reverse possibility would tend to make the positive short-wavelength part of the MCD spectrum broad and the long-wavelength part narrow. In view of the broadness of the spectra a more extensive or detailed analysis of the cyclohexane spectra is not possible.[15] However it is worthwhile to note that Mg atoms isolated in noble-gas matrices reveal similar MCD and absorption features with more detail for the $^1S_0(3s^2) \rightarrow {}^1P_1(3s3p)$ transition.[12] A moment analysis of MCD and absorption assuming an octahedral environment showed a dominant contribution to the bandwidth from noncubic (Jahn-Teller-active) modes. Similar conclusions were reached from detailed analyses of absorption and MCD spectra for Li and Na atoms in noble-gas matrices, where the transitions $^2S(ns^1) \rightarrow {}^2p(np^1)$ were studied.[13,14] A careful analysis of the MCD for matrix-isolated Hg is a logical extension of this work and is planned in the future.

Acknowledgment. Helpful discussions with Dr. C. T. Lin are gratefully acknowledged.

Registry No. Hg, 7439-97-6; NCMe, 75-05-8; H_2O, 7732-18-5; cyclohexane, 110-82-7.

(12) Mowery, R. L.; Miller, J. C.; Krausz, E. R.; Schatz, P. N.; Jacobs, S. M.; Andrews, L. *J. Chem. Phys.* **1979**, *70*, 3920.
(13) Lund, P. A.; Smith, D.; Jacobs, S. M.; Schatz, P. N. *J. Phys. Chem.* **1984**, *88*, 31.
(14) Rose, J.; Smith, D.; Williamson, B. E.; Schatz, P. N.; O'Brien, M. C. M. *J. Phys. Chem.* **1986**, *90*, 2608.
(15) A reviewer has offered an alternative suggestion that the unsymmetrical shape of the solution spectra may arise from transitions to a distorted potential surface that is due to vibronic coupling of the solvent cage modes with the Hg atom excited state.

Contribution from the Lehrstuhl für Anorganische Chemie I der Ruhr-Universität, D-4630 Bochum, FRG, Institut für Anorganische Chemie der Johann-Wolfgang-Goethe-Universität, D-6000 Frankfurt/Main, FRG, and Max-Planck-Institut für Strahlenchemie, D-4330 Mülheim an der Ruhr, FRG

Redox Reactivity of Bis(1,4,7-triazacyclononane)iron(II/III) Complexes in Alkaline Solution and Characterization of a Deprotonated Species: Amidoiron(III) vs Aminyliron(II) Ground-State Formulation. EPR, Kinetic, Pulse Radiolysis, and Laser Photolysis Study

Klaus Pohl,[1a] Karl Wieghardt,*[1a] Wolfgang Kaim,[1b] and Steen Steenken[1c]

Received July 30, 1987

The redox reactivity of the low-spin complexes $[FeL_2]^{3+}$ and $[FeL_2]^{2+}$ (L = 1,4,7-triazacyclononane, $C_6H_{15}N_3$) in alkaline aqueous solution has been investigated. Orange $[Fe^{III}L_2]^{3+}$ is reversibly deprotonated ($pK_a = 11.4 \pm 0.4$) in alkaline solution to yield a deep blue species ($\lambda_{max} = 542$ nm; $\epsilon = 1.8 \times 10^3$ M^{-1} cm^{-1}), which has been characterized by its frozen-solution EPR spectrum as the low-spin amidoiron(III) complex, $[Fe^{III}L(L\text{-}H)]^{2+}$ ((L-H) is the N-deprotonated form of the ligand L). The aminyl radical iron(II) formulation, $[Fe^{II}L(^{\bullet}L\text{-}H)]^{2+}$, is proposed to be an electronically excited state (ligand-to-metal charge transfer). $[Fe^{III}L(L\text{-}H)]^{2+}$ disproportionates slowly under anaerobic conditions to yield 50% $[Fe^{II}L_2]^{2+}$ and probably 50% $[LFe^{II}(OH_2)_3]^{2+}$ and a two-electron-oxidation product of one 1,4,7-triazacyclononane ligand, which has not been characterized. In the presence of an external oxidant (H_2O_2 or oxygen) the blue species decomposes to produce quantitatively 1 equiv of oxidized macrocycle and $[Fe^{III}L(OH_2)_3]^{3+}$. The kinetics of both reactions have been measured. Pulse radiolysis experiments have shown that the oxidation of $[FeL_2]^{2+}$ with $Br_2^{\bullet-}$, $I_2^{\bullet-}$, and $(SCN)_2^{\bullet-}$ and oxygen-centered radicals such as $OH^{\bullet}$ and the phenoxyl radical yield $[Fe^{III}L_2]^{3+}$ at nearly diffusion controlled rates in the pH range 4-10. At higher pH values (11-13) the blue amidoiron(III) species is formed. $[Fe^{III}L(L\text{-}H)]^{2+}$ oxidizes ascorbate(2-) to give $[Fe^{II}L_2]^{2+}$ and the ascorbate(1-) radical. Laser photolysis of solutions of $[FeL_2]^{2+}$ at pH 8-10 with 20-ns pulses from a KrF excimer laser ($\lambda = 248$ nm) produces $[FeL_2]^{3+}$ and the hydrated electron with a quantum yield of 0.9; at pH >10 $[FeL(L\text{-}H)]^{2+}$ and $e^-(aq)$ are produced at the same rate.

Introduction

We have recently reported the synthesis and spectroscopic properties of two low-spin iron(III) and iron(II) complexes, each of them containing two molecules of the cyclic tridentate ligand 1,4,7-triziacyclononane (L).[2] These were examples of low-spin iron(II/III) complexes in an octahedral environment of six saturated amine nitrogen atoms. The structures of $[FeL_2]Cl_2 \cdot 4H_2O$ and $[FeL_2]Cl_3 \cdot 5H_2O$ were subsequently determined by X-ray crystallography.[3] $[FeL_2]^{2+}$ is remarkably stable in aqueous solution in the pH range 6-13. No ligand dissociation has been observed at 25 °C for 6 h. The same was found to be true for orange $[FeL_2]^{3+}$ in the pH range 2-10, but at pH >10 a dramatic color change of such solutions to deep blue is observed. This color change is completely reversible; reacidification restores quantitatively the $[FeL_2]^{3+}$ species.

In this paper we describe the nature of this blue species and the redox properties of $[FeL_2]^{3+}$ and $[FeL_2]^{2+}$. As we will show, the blue species is the monodeprotonated form of $[FeL_2]^{3+}$; we will abbreviate the N-deprotonated form of the parent ligand 1,4,7-triazacyclonoane as (L-H), $(C_6H_{14}N_3)^-$. One of the questions to be answered is the problem of the electronic ground state of this blue species; i.e., are we dealing with an amidoiron(III) or, alternatively, an aminyliron(II) radical dication?

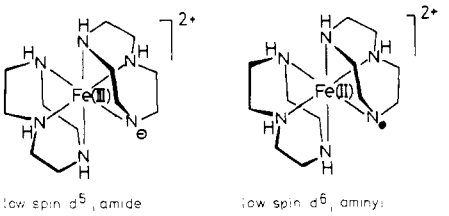

low spin d^5, amide low spin d^6, aminyl

Species like this have been postulated as reactive intermediates

(1) (a) Ruhr-Universität Bochum. (b) Universität Frankfurt. (c) Max-Planck-Institut Mülheim an der Ruhr.
(2) Wieghardt, K.; Schmidt, W.; Herrmann, W.; Küppers, H. J. *Inorg. Chem.* **1983**, *22*, 2953.
(3) Boeyens, J. C. A.; Forbes, A. G. S.; Hancock, R. D.; Wieghardt, K. *Inorg. Chem.* **1985**, *24*, 2926.

0020-1669/88/1327-0440$01.50/0

in the metal-induced dehydrogenation of saturated amine ligands to yield coordinated imine or diimine ligands,[4] but it has not been possible previously to characterize a complex of this type. Oxidative dehydrogenation of amines coordinated to Ru(III),[7,15] Fe(III),[4-6,16,20] Ni(II),[21-25] Cu(II),[26] Co(II),[24] and Os(IV)[28] has been observed.

The present system is unique in the respect that the deprotonated species is relatively stable in alkaline solution. The disproportionation reaction under anaerobic conditions and in the absence of other external oxidants is slow. This allows a spectroscopic investigation of the monodeprotonated form. The formation of an iminoiron(II) species is hampered because of the steric requirements of the coordinated nine-membered triamine, which upon two-electron oxidation yields a highly strained coordinated cyclic imine–diamine ligand. This ligand most probably hydrolyzes rapidly with concomitant ring opening and dissociation of the open-chain ligand (loss of the macrocyclic effect).

Experimental Section

The ligand 1,4,7-triazacyclononane has been prepared by the Richman and Atkins procedure as described previously.[29]

$[FeL_2]Br_3 \cdot 5H_2O$, $[FeL_2]Br_2 \cdot 3H_2O$, $[FeL_2]Cl_3 \cdot 5H_2O$, and $[FeL_2]Cl_2 \cdot 4H_2O$ have been prepared previously.[2,3] For the present study the perchlorate salts were prepared.

Caution! Perchlorate salts are potentially hazardous, especially when heated.

$[FeL_2](ClO_4)_2$. To an argon-scrubbed saturated aqueous solution of ammonium acetate (20 mL) was added $FeCl_2 \cdot 4H_2O$ (0.5 g, 2.5 mmol) and a 1 M ethanolic solution (5 mL) containing the ligand 1,4,7-triazacyclononane. This solution turned blue within 10 min at room temperature. Addition of sodium perchlorate (3 g at 4 °C) initiated the precipitation of transparent pale blue crystals, which were filtered off, washed with cold ethanol and ether, and dried under argon (yield 1.2 g, 92%). Anal. Calcd for $Fe(C_6H_{15}N_3)_2(ClO_4)_2$: C, 28.0; H, 5.8; N, 16.3; Fe, 10.9; ClO_4, 38.9. Found: C, 28.0; H, 5.9; N, 16.4; Fe, 10.8; ClO_4, 38.8.

$[FeL_2](ClO_4)_3$. $[FeL_2](ClO_4)_2$ (0.4 g) was dissolved in a 0.5 M aqueous solution of ammonium acetate (30 mL), and the mixture was stirred in the presence of oxygen for 3 h at room temperature. To the then yellow-orange solution was added sodium perchlorate (2 g), initiating at 4 °C the precipitation of orange crystals, which were filtered off, washed with ethanol and ether, and air-dried (yield 0.46 g, 96%). Anal. Calcd for $Fe(C_6H_{15}N_3)_2(ClO_4)_3$: C, 23.4; H, 4.9; N, 13.7; Fe, 9.1. Found: C, 23.5; H, 4.8; N, 13.7; Fe, 9.5.

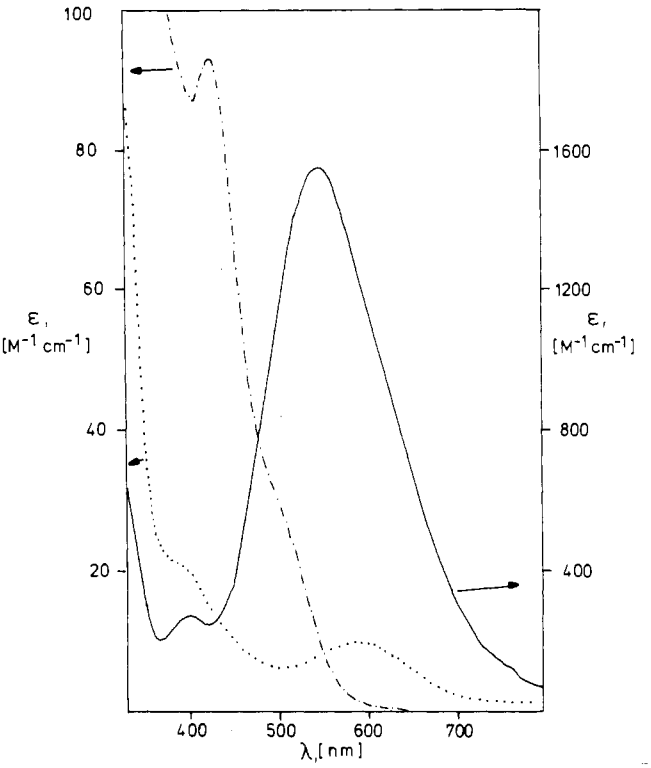

Figure 1. Electronic spectra: (a) $[Fe^{III}L_2]^{3+}$ in aqueous solution (20 °C) (–·–); (b) $[Fe^{III}L(L\text{-}H)]^{2+}$ species ($[FeL_2]^{3+}$ in 1 M NaOH; 20 °C) (—); (c) $[Fe^{II}L_2]^{2+}$ in aqueous solution (20 °C) (···).

Scheme I

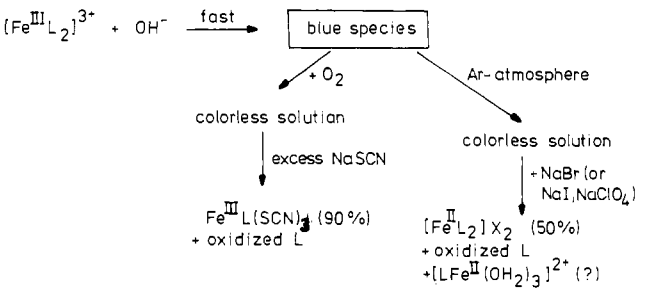

Instrumentation. The laser experiments were performed with a Lambda Physik EMG 103 MSC excimer laser that delivered pulses at 248.5 nm (KrF) of ~20-ns duration. The pulse intensity of the laser light was varied between 20 and 200 mJ by using 230-nm cutoff filters. The laser was interfaced with a DEC LSI-11/73 computer, which also ran the optical and conductance detection systems and was used for the analysis and documentation of the data.

The pulse radiolysis experiments were performed with a 3-MeV Van de Graaff accelerator as described previously.[30]

The UV–vis spectra were recorded on a Perkin-Elmer Lambda 9 spectrophotometer and the ESR spectra on a Varian E9 instrument in the X band (9.5 GHz); for calibration and g-value determination the perylene anion radical in 1,2-dimethoxyethane was used.

The apparatus used for cyclic voltammetric measurements has been described previously.[2]

Results

Preliminary Observations. Both $[FeL_2]^{3+}$ and $[FeL_2]^{2+}$ are kinetically stable in aqueous solution at 25 °C (pH ~7) for at least 3 h. No formation of precipitates and no spectral changes have been observed during this period of time. $[FeL_2]^{2+}$ is stable even in alkaline aqueous solution (pH ~12) toward ligand dissociation under anaerobic conditions. Addition of sodium hy-

(4) Ferreira, A. M. C.; Toma, H. E. *J. Chem. Soc., Dalton Trans.* **1983**, 2051.
(5) Toma, H. E.; Ferreira, A. M. C.; Iha, N. Y. M. *Nouv. J. Chim.* **1985**, *9*, 473.
(6) Goto, M.; Takeshita, M.; Kanda, N.; Sakai, T.; Goedken, V. L. *Inorg. Chem.* **1985**, *24*, 582.
(7) Ridd, M. J.; Keene, F. R. *J. Am. Chem. Soc.* **1981**, *103*, 5733.
(8) Keene, F. R.; Ridd, M. J.; Snow, M. R. *J. Am. Chem. Soc.* **1983**, *105*, 7075.
(9) McWhinnie, W. R.; Miller, J. D.; Watts, J. B.; Waddan, D. Y. *J. Chem. Soc. D* **1971**, 629.
(10) Lane, B. C.; Lester, J. E.; Basolo, F. *J. Chem. Soc., Chem. Commun.* **1971**, 1618.
(11) Mahoney, D. F.; Beattie, J. K. *Inorg. Chem.* **1973**, *12*, 2561.
(12) Alvarey, V. E.; Allen, R. J.; Matsubara, T.; Ford, P. C. *J. Am. Chem. Soc.* **1974**, *96*, 7686.
(13) Keene, R. F.; Salmon, D. J.; Meyer, T. J. *J. Am. Chem. Soc.* **1976**, *98*, 1884.
(14) Brown, G. M.; Weaver, T. R.; Keene, F. R.; Meyer, T. J. *Inorg. Chem.* **1976**, *15*, 190.
(15) Diamond, S. E.; Tom, G. M.; Taube, H. *J. Am. Chem. Soc.* **1975**, *97*, 2661.
(16) Goedken, V. L.; Busch, D. H. *J. Am. Chem. Soc.* **1972**, *94*, 7355.
(17) Goedken, V. L. *J. Chem. Soc., Chem. Commun.* **1972**, 207.
(18) Dabrowiak, J. C.; Busch, D. H. *Inorg. Chem.* **1975**, *14*, 1881.
(19) Watkins, D. D.; Riley, D. P.; Stone, J. A.; Busch, D. H. *Inorg. Chem.* **1976**, *15*, 387.
(20) Tait, A. M.; Busch, D. H. *Inorg. Chem.* **1976**, *15*, 197.
(21) Curtis, N. F. *J. Chem. Soc.* **1960**, 4409.
(22) Vassian, E. G.; Murmann, R. K. *Inorg. Chem.* **1967**, *6*, 2043.
(23) Barefield, E. K.; Busch, D. H. *Inorg. Chem.* **1971**, *10*, 109.
(24) Hipp, G. J.; Lindoy, L. F.; Busch, D. H. *Inorg. Chem.* **1972**, *11*, 1988.
(25) Barefield, E. K.; Mocella, M. T. *J. Am. Chem. Soc.* **1975**, *97*, 4238.
(26) Olsen, D. C.; Vasitevskis, J. *Inorg. Chem.* **1971**, *10*, 463.
(27) Tang, S. C.; Holm, R. H. *J. Am. Chem. Soc.* **1975**, *97*, 3359.
(28) Lay, P. A.; Sargeson, A. M.; Skelton, B. W.; White, A. H. *J. Am. Chem. Soc.* **1982**, *104*, 6161.
(29) (a) Richman, J. E.; Atkins, T. J. *J. Am. Chem. Soc.* **1974**, *96*, 2268. (b) Wieghardt, K.; Schmidt, W.; Nuber, B.; Weiss, J. *Chem. Ber.* **1979**, *112*, 2220.
(30) Jagannadham, V.; Steenken, S. *J. Am. Chem. Soc.* **1984**, *106*, 6542.

droxide to an orange aqueous solution of $[FeL_2]^{3+}$ leads to an immediate color change to deep blue-violet; reacidification yields again the original yellow-orange solution. This process may be repeated several times within 20 min without losing intensity of the observed bands in the visible region of either the yellow $[FeL_2]^{3+}$ or blue species. The reaction is completely reversible, and equilibrium is reached rapidly. Electronic spectra of both species are shown in Figure 1a,b. Addition of NaOH to an aqueous solution of $[FeL_2]^{2+}$, which is nearly colorless, does not change the electronic spectrum (Figure 1c).

Alkaline, blue-violet solutions of $[FeL_2]^{3+}$ decompose slowly under anaerobic conditions (2–3 h at 25 °C), and eventually a colorless solution is obtained. Upon addition of sodium iodide, sodium bromide, or sodium perchlorate the precipitation of $[FeL_2]I_2$, $[FeL_2]Br_2$, or $[FeL_2](ClO_4)_2$ was initiated, which allowed the recovery of 44% of the original iron(III) complex as $[FeL_2]^{2+}$. Taking into account a small solubility of these salts, we assume that half of the starting material, 50% of $[FeL_2]^{3+}$, is converted to $[FeL_2]^{2+}$ during the above reaction. We have not been able to identify any other reaction products. Thus, the presumed oxidation product of one 1,4,7-triazacyclononane ligand has not been characterized. The electronic spectrum of the decolorized solution is identical with that of a geniune solution containing $[FeL_2]^{2+}$ (half of the starting iron(III) content).

Under aerobic conditions the decolorization of the blue-violet solution is much faster. Addition of sodium isothiocyanate to such a solution yields quantitatively a precipitate of the red, neutral complex $LFe^{III}(NCS)_3$, which has been characterized previously.[31] A total of 90% of the starting $[FeL_2]^{3+}$ was thus converted to $LFe(NCS)_3$. Again the ligand oxidation product has not been identified.

Thus, the overall stoichiometry of the decomposition of the blue species is different under aerobic and anaerobic conditions (Scheme I). We suggest that oxidation of one coordinated, deprotonated macrocycle occurs via two distinct reaction paths.

Determination of the Acid Dissociation Constant of $[FeL_2]^{3+}$. Potentiometric titrations of $[FeL_2]Br_3 \cdot 5H_2O$ (0.7–1.6 mmol) dissolved in 50 mL of 0.1 M KNO_3 at 25 °C with 2 M sodium hydroxide revealed that only one proton per $[FeL_2]^{3+}$ is released and the acid dissociation constant $pK_a = 11.4 \pm 0.2$ was determined:

$$[FeL_2]^{3+} \overset{K_a}{\rightleftharpoons} [FeL(L\text{-}H)]^{2+} + H^+ \qquad (1)$$

Since a veritable color change from orange to deep blue occurs during these titrations, we have also determined the pK_a value spectrophotometrically following the change of absorption at 545 nm, where only the deprotonated species absorbs strongly ($\epsilon = 1.8 \times 10^3$ L mol^{-1} cm^{-1}), as a function of pH. A value of 11.8 ± 0.4 was determined at 25 °C ($I = 0.1$ M).

The pK_a value was also determined more indirectly by three further independent techniques: (i) laser photolysis of $[FeL_2]^{2+}$ as a function of pH ($pK_a = 11.7 \pm 0.1$); (ii) pulse radiolysis experiments oxidizing $[FeL_2]^{2+}$ with $Br_2^{\bullet-}$, $I_2^{\bullet-}$, and $(SCN)_2^{\bullet-}$ ($pK_a = 11.1 \pm 0.1$); (iii) cyclic voltammetry ($pK_a = 11$–12). These experiments will be described in detail below. All these different techniques yield a pK_a value of 11.4 ± 0.4.

Electronic and EPR Spectra of Complexes. Diamagnetic $[FeL_2]^{2+}$ has the ground term $^1A_{1g}$, and two low-lying spin-allowed transitions to $^1T_{1g}$ and $^1T_{2g}$ are observed at 588 nm ($\epsilon = 10$ L mol^{-1} cm^{-1}) and 384 nm (sh) (Figure 1c), respectively. Low-spin $[FeL_2]^{3+}$ has a ground state of $^2T_{2g}$ in an octahedral field; two bands at 427 nm ($\epsilon = 91$) and 515 nm (sh) are observed and may be due to d–d transitions rather than the usual charge-transfer (CT) bands observed for low-spin Fe(III) complexes (Figure 1a).

Figure 1b shows the electronic spectrum of $[FeL_2]^{3+}$ in 1 M sodium hydroxide. The spectrum is dominated by a very intense CT band at 545 nm ($\epsilon = 1.8 \times 10^3$) and a weaker band at 396 nm ($\epsilon = 274$). The given intensity is a corrected value taking into account the decomposition of the blue species during the period of time after mixing the solution of $[FeL_2]^{3+}$ with NaOH and recording the spectrum.

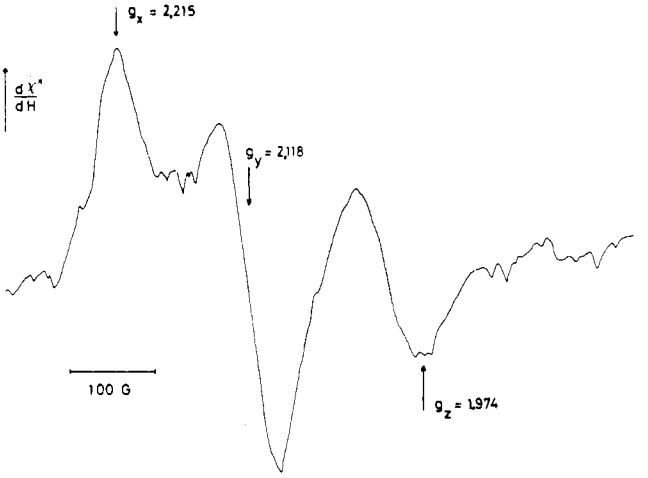

Figure 2. EPR spectrum of a saturated frozen solution of $[FeL_2]^{3+}$ in an ethanol/water mixture (1:1) containing 1 M KOH in the temperature range −100 to −150 °C.

A saturated aqueous (or dimethylformamide) solution of orange $[FeL_2]^{3+}$ does not show a measurable EPR signal in the temperature range 100–298 K. As mentioned above, low-spin iron(III) complexes have a $^2T_{2g}$ ground state in O_h symmetry. However, orbital splitting by lower symmetry and spin–orbit coupling typically produces several excited states close to the doublet ground state, which are responsible for fast spin–lattice relaxation and very broad signals, except at very low temperatures.[32]

This situation changes quite dramatically upon deprotonation of $[FeL_2]^{3+}$ in alkaline aqueous solution or in dimethylformamide (DMF)/potassium *tert*-butoxide. The EPR spectrum of the latter blue solution at room temperature exhibits a single EPR signal at $g = 2.112$ ($\Delta H_{pp} = 48$ G). A similar spectrum was obtained in 1 M NaOH. In frozen alkaline (KOH) water/ethanol mixtures (123–173 K) this signal is split into the three principal components of the g tensor: $g_1 = 2.215$, $g_2 = 2.118$, and $g_3 = 1.975$ (Figure 2). The intensity of these EPR signals decreases at the same rate as the decomposition of the blue species occurs.

The relatively small[34] anisotropy of the blue species and the rather small EPR line width at room temperature in DMF are quite remarkable when compared with those of other low-spin iron(III) complexes with nitrogen ligands;[32] such spectroscopic features are more typical of iron(III) complexes with a sulfur donor set[33] or organometallic d^5 low-spin systems involving Fe(III),[34] Mn(II),[35] or V(0).[36] These special properties of the blue species relative to those of its precursor are due to amido ion formation at one 1,4,7-triazacyclononane ligand by deprotonation. As very powerful nucleophiles, amides can induce a very strong splitting fo the ligand field levels; they create much more favorable relaxation conditions for the observation of EPR spectra.

Similar observations have recently been reported for the low-spin manganese(II) complexes $Cp(CO)_2MnL$,[35] where EPR signals could only be observed at room temperature with strong, negatively charged ligands L such as amides,[35–37] alkoxides,[38] thiolates, or

(31) Wieghardt, K.; Pohl, K.; Ventur, D. *Angew. Chem., Int. Ed. Engl.* **1985**, *24*, 392.
(32) Bencini, A.; Gatteschi, D. In *Transition Metal Chemistry*; Melson, G. A., Figgis, B. N., Eds.; Marcel Dekker: New York, 1982; Vol. 8, p 1.
(33) (a) Knauer, K.; Hemmerich, P.; van Voorst, J. D. W. *Angew. Chem.* **1967**, *79*, 273; *Angew. Chem., Int. Ed. Engl.* **1967**, *6*, 262. (b) Cotton, F. A.; Gibson, J. F. *J. Chem. Soc. A* **1971**, 803.
(34) Elschenbroich, C.; Bilger, E.; Ernst, R. D.; Wilson, D. R.; Kralik, M. S. *Organometallics* **1985**, *4*, 2068.
(35) Gross, R.; Kaim, W. *Angew. Chem.* **1985**, *97*, 869; *Angew. Chem., Int. Ed. Engl.* **1985**, *24*, 856.
(36) Bratt, S. W.; Kassyk, A.; Perutz, R. N.; Symons, M. C. R. *J. Am. Chem. Soc.* **1982**, *104*, 490.
(37) (a) Sellmann, D.; Müller, J.; Hofmann, P. *Angew. Chem.* **1982**, *94*, 708; *Angew. Chem., Int. Ed. Engl.* **1982**, *21*, 691. (b) Sellmann, D.; Müller, J. *J. Organomet. Chem.* **1985**, *281*, 249.
(38) Gross, R.; Kaim, W. *Inorg. Chem.* **1987**, *26*, 3596.

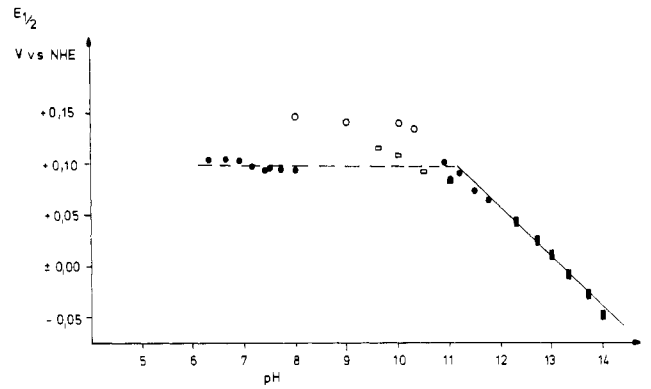

Figure 3. pH dependence of the redox potential of the couple $[FeL_2]^{3+/2+}$ at 25 °C (I = 0.1 M) measured by cyclic voltammetry at a hanging-mercury-drop electrode: (●) $H_2PO_4^-/HPO_4^{2-}/OH^-$; (■) NaOH; (□) HCO_3^-/OH^-; (○) borate/OH^-.

selenides[39] and not with weak ligands such as amines, carbonyl compounds, or phosphanes.[40]

Superhyperfine splitting from ^{14}N or ^1H nuclei as reported for a paramagnetic nickel–cyclam complex[25] or for a few Cp-$(CO)_2$MnL species[35] could not be detected for the present blue species and must be smaller than 2.5 mT.

In conclusion, the ground state of the blue species must be described as an amidoiron(III) complex according to the EPR results. The aminyliron(II) radical formulation[37] is appropriate only for the LMCT excited state.[35]

Electrochemistry. The cyclic voltammogram of $[FeL_2]^{3+}$ in 0.1 M $LiClO_4$ exhibits one wave in the potential range +1.0 to −1.5 V vs Ag/AgCl. The peak-to-peak separation of 60 mV and an i_{pa}/i_{pc} ratio of 1.0, both independent of the scan rate (20–200 mV s^{-1}), indicate the electrochemical reversibility of the one-electron redox process (eq 2).[2] We have now investigated the pH de-

$$[FeL_2]^{3+} + e^- \rightleftarrows [FeL_2]^{2+} \quad (2)$$

pendence of the redox potential at 25 °C with variety of different buffers (I = 0.1 M), e.g. $H_2PO_4/HPO_4^{2-}/OH^-$, HCO_3^-/OH^-, and borate/OH^-, and in solutions containing known amounts of sodium hydroxide. Figure 3 shows the pH dependence measured at a hanging-mercury-drop electrode. In the pH range 7–10 there is a small but significant dependence of the redox potential on the nature of the buffer used. Oxoanions such as phosphate, carbonate, and borate as well as their various protonated forms are known to form ion pairs with cationic amine complexes via strong hydrogen bonding, which is believed to be the cause for the observed dependence. At pH >10 there is a linear shift to more cathodic potentials of the redox potential with increasing pH. The slope of −60 mV/pH unit is in excellent agreement with the theoretical value of −59 mV/pH unit assuming Nernstian behavior and the transfer of one electron and one proton to the deprotonated form of $[FeL_2]^{3+}$ to produce $[FeL_2]^{2+}$. The acid dissociation constant of $[FeL_2]^{3+}$ is found from these measurements to be pK_a = 11–12, in reasonable agreement with the other determinations.

Kinetics of the Decomposition of the Amidoiron(III) Species. The rate of the slow decomposition of the blue amidoiron(III) species in anaerobic, alkaline aqueous solution was followed spectrophotometrically at 545 nm and 25 °C as a function of pH. Deaerated solutions of $[FeL_2]^{3+}$ (2×10^{-4} M) were mixed with a known amount of sodium hydroxide dissolved in degassed water. $[OH^-]$ was varied between 6×10^{-3} and 0.5 M. For the following let $[Fe_{tot}]$ be the sum of $[Fe^{III}L(L\text{-}H)^{2+}]$ and $[FeL_2^{3+}]$ present in the solution. $[FeL(L\text{-}H)^{2+}]_{t=0}[FeL(L\text{-}H)^{2+}]_t^{-1}$ is obtained as the ratio of the absorbances at 545 nm observed at the beginning and after time t, respectively. Plots of $[FeL(L\text{-}H)^{2+}]_{t=0}$ $[FeL(L\text{-}H)^{2+}]_t^{-1}[Fe_{tot}]^{-1}$ vs time were linear for 4 half-lives with the exception of two experiments at $[OH^-]$ = 0.5 and 0.25 M, where deviation from linearity occurred after approximately 3 half-lives:

$$\frac{[FeL(L\text{-}H)^{2+}]_{t=0}}{[FeL(L\text{-}H)^{2+}]_t}\frac{1}{[Fe_{tot}]_{t=0}} = k_{obsd}t + \frac{1}{[Fe_{tot}]_{t=0}} \quad (3)$$

A plot of the reciprocals of k_{obsd} at various $[OH^-]$ vs $[H^+]$ (calculated from $[OH^-]$) again was found to be linear (Figure 4):

$$\frac{1}{k_{obsd}} = \frac{[H^+]}{k_1K_{exptl}} + \frac{1}{k_1} = \frac{1}{k_1}\left(\frac{[H^+]}{K_{exptl}} + 1\right) \quad (4)$$

Numerical values for k_1 of 7.6 M^{-1} s^{-1} and for K_{exptl} of $10^{-12.1}$ M were obtained from the intercept and slope of Figure 4. From the definitions of K_a and $[Fe_{tot}]$

$$K_a = [FeL(L\text{-}H)^{2+}][H^+]/([Fe_{tot}] - [FeL(L\text{-}H)^{2+}])$$

and hence

$$\frac{[H^+]}{K_a} + 1 = \frac{[Fe_{tot}]}{[FeL(L\text{-}H)^{2+}]} \quad (5)$$

Since the value for K_{exptl} of $10^{-12.1}$ within error limits agrees with the K_a value of $10^{-11.4}$ found by potentiometric and spectroscopic titrations, $K_{exptl} = K_a$.

Hence, from eq 4 and 5

$$k_{obsd} = k_1\frac{[Fe(L\text{-}H)^{2+}]}{[Fe_{tot}]} \quad (6)$$

Insertion into (3) gives

$$[FeL(L\text{-}H)^{2+}]_t^{-1} = k_1t + [FeL(L\text{-}H)^{2+}]_{t=0}^{-1}$$

and differentiation of this equation gives eq 7. This rate law and

$$-d[FeL(L\text{-}H)^{2+}]/dt = k_1[FeL(L\text{-}H)^{2+}]^2 \quad (7)$$

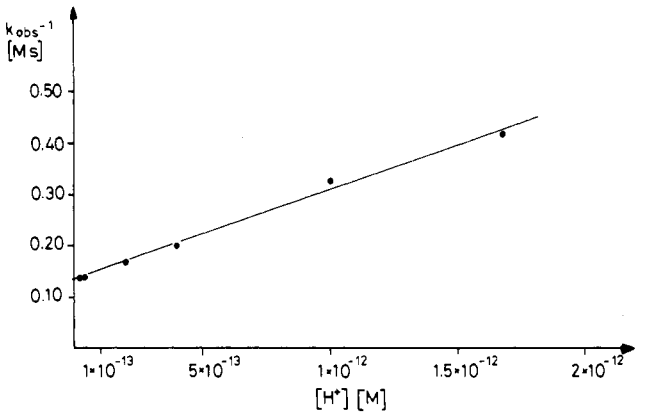

Figure 4. Dependence of the reciprocal second-order rate constant of the anaerobic disproportionation of $[FeL_2]^{3+}$ on $[H^+]$ at 25 °C (I = 0.5 M; $[Fe^{III}]_{tot} = 2 \times 10^{-4}$ M).

Scheme II

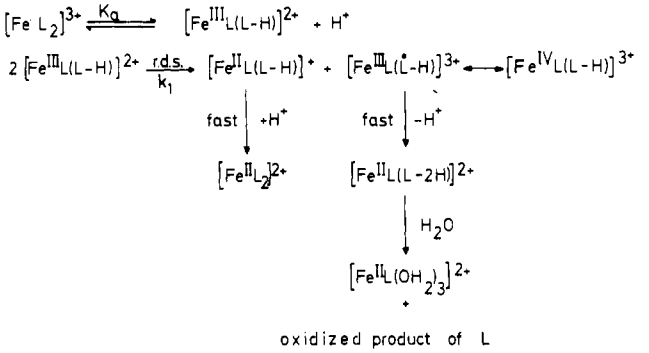

(39) (a) Winter, A.; Huttner, G.; Zsolnai, L.; Kroneck, P.; Gottlieb, M. *Angew. Chem.* **1984**, *96*, 986; *Angew. Chem., Int. Ed. Engl.* **1984**, *23*, 975. (b) Winter, A.; Huttner, G.; Gottlieb, M.; Jibril, I. *J. Organomet. Chem.* **1985**, *286*, 317.

(40) Gross, R. Ph.D. Thesis, Universität Frankfurt, 1986.

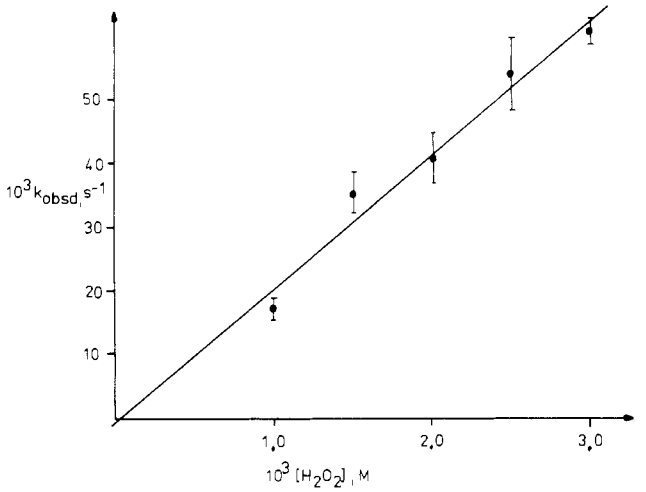

Figure 5. Dependence of the rate of the decay of blue $[Fe^{III}L(L\text{-}H)]^{2+}$ on $[H_2O_2]$ at 25 °C at $[OH^-]$ = 0.25 M = constant (I = 0.5 M).

the product analysis are consistent with the mechanism indicated in Scheme II.[52]

We have also studied the decomposition reaction in the presence of H_2O_2 as external oxidant. $[FeL_2]^{3+}$ and excess H_2O_2 (0.1 M) in the pH range 7–9 is stable for at least 3–4 h; no reaction occurs at 25 °C. If the pH is raised to >10, the solution becomes deep blue; the blue amidoiron(III) species is formed as was judged from its typical absorption spectrum. The blue fades quite rapidly in the presence of H_2O_2, and upon addition of thiocyanate red $LFe(NCS)_3$ precipitated essentially quantitatively (on the basis of initial $[Fe^{III}]$). Thus, the reaction of $[FeL_2]^{3+}$ and H_2O_2 in alkaline solution effectively oxidizes one 1,4,7-triazacyclononane ligand per $[FeL_2]^{3+}$. The reaction was monitored spectrophotometrically at 545 nm as a function of time. At 25 °C and $[OH^-]$ = constant = 0.25 M (I = 0.5 M) the concentration of H_2O_2 was varied between 1×10^{-3} and 3×10^{-3} M ($[FeL_2^{3+}] = 1 \times 10^{-4}$ M). Plots of ln $(A_t - A_\infty)$ vs time were linear for 3–4 half-lives. Figure 5 shows a plot of the observed pseudo-first-order rate constant vs $[H_2O_2]$. The rate law is of the form shown in eq 8 with $k_{H_2O_2} = 21.2 \pm 0.4$ M^{-1} s^{-1} at 25 °C.

$$k_{obsd} = k_{H_2O_2}[H_2O_2] \quad (8)$$

Finally, we have measured the kinetics of the reaction between $[FeL_2]^{2+}$ and H_2O_2. In the pH range 7.5–9.1 $[FeL_2]^{3+}$ is produced according to eq 9. The rate of the reaction was found to be

$$2[FeL_2]^{2+} + H_2O_2 \rightarrow 2[FeL_2]^{3+} + 2OH^- \quad (9)$$

independent of $[H^+]$ in the pH range employed. The final spectrum after the reaction is completed corresponds to that of $[FeL_2]^{3+}$. A simple second-order rate law (eq 10) was found with

$$d[FeL_2^{3+}]/dt = -d[FeL_2^{2+}]/dt = k[FeL_2^{2+}][H_2O_2] \quad (10)$$

$k = 0.45 \pm 0.02$ M^{-1} s^{-1} at 25 °C (pH 8.4; I = 0.5 M). At pH <7 a significant increase in the rate is observed. Rapid acid-induced ligand dissociation processes of $[FeL_2]^{2+}$ probably produce iron(II) species, which are stronger reductants than $[FeL_2]^{2+}$.

The mechanism of the oxidation of $[FeL_2]^{2+}$ by H_2O_2 is most probably an outer-sphere one-electron-transfer process in the rate-determining step with successive rapid reduction of the $OH^\bullet$ radical intermediate by a second $[FeL_2]^{2+}$ (eq 11 and 12). Since

$$[FeL_2]^{2+} + H_2O_2 \xrightarrow{k} [FeL_2]^{3+} + OH^\bullet + OH^- \quad (11)$$

$$[FeL_2]^{2+} + OH^\bullet \xrightarrow{fast} [FeL_2]^{3+} + OH^- \quad (12)$$

$[FeL_2]^{2+}$ has no labile coordination site available, an inner-sphere-type mechanism is not considered to be likely. It is noted that in addition to simple outer-sphere electron transfer in reaction 12 abstraction from the ligand of 10% of the hydrogens probably occurs. This has been established by pulse radiolysis experiments (see below).

Table I. Second-Order Rate Constants for the Reaction of $[FeL_2]^{2+}$ with Oxidizing Radicals at 25 °C (pH 4–13)

radical	$10^{-9}k$, M^{-1} s^{-1}	radical	$10^{-9}k$, M^{-1} s^{-1}
$I_2^{\bullet-}$	6.4	$OH^\bullet$	6.4
$(SCN)_2^{\bullet-}$	5.9	$PhO^\bullet$	2.4
$Br_2^{\bullet-}$	6.3		

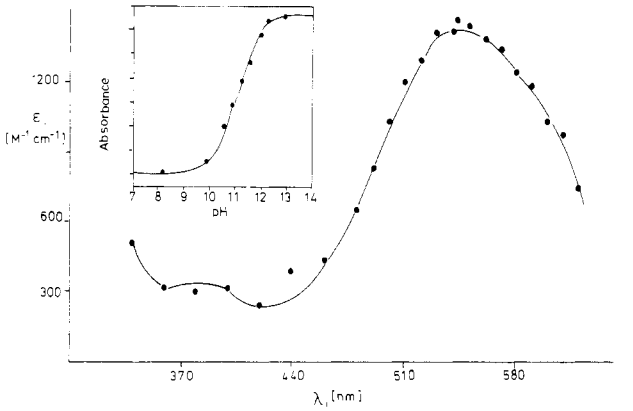

Figure 6. Spectrum of the reaction product measured after completion of reaction 13 at pH 13. Inset: optical density as a function of pH for reaction 13.

Pulse Radiolysis Experiments. When N_2O-saturated aqueous solutions containing 10 mM X^- (X^- = Br^-, I^-, SCN^-) are irradiated, the radical anions $X_2^{\bullet-}$ are formed within ≤0.1 μs.[41] In the absence of other suitable reactants these radicals decay by diffusion-controlled bimolecular reactions. At an initial radical concentration of 1–2 μM the first half-life for this reaction is in the millisecond time scale.

In solutions that contained 10 mM X^- the lifetime of $X_2^{\bullet-}$ was drastically reduced in the presence of $[FeL_2]^{2+}$. At concentrations of $[FeL_2]^{2+}$ between 0.1 and 0.5 mM the decay of $X_2^{\bullet-}$ obeyed a first-order rate law and the decay rates increased linearly with $[FeL_2^{2+}]$. From these dependencies the bimolecular rate constants for reaction of $X_2^{\bullet-}$ with $[FeL_2]^{2+}$ were obtained as (6–9) × 10^9 M^{-1} s^{-1} (Table I). These rate constants were found to be independent of pH in the range 4–13. After completion of the decay reactions of $X_2^{\bullet-}$ (i.e. after 20 μs) the spectra measured at pH <10 were identical with that of $[FeL_2]^{3+}$ (Figure 1a). The reaction between $X_2^{\bullet-}$ and $[FeL_2]^{2+}$ is thus seen to yield the one-electron-oxidation product $[FeL_2]^{3+}$ (eq 13). When reaction 13 was

$$X_2^{\bullet-} + [FeL_2]^{2+} \xrightarrow{pH\ 4-10} 2X^- + [FeL_2]^{3+} \quad (13)$$

performed at pH values >10, a species with an intense absorption at 542 nm was formed (Figure 6). The optical density measured at 542 nm increased with increasing pH in a sigmoidal form up to a plateau at pH ~13 (inset of Figure 6). The inflection point of this titration curve is at pH 11.6. With respect to λ_{max} (542 nm) and ϵ (1.8×10^3 M^{-1} cm^{-1}) the spectrum of this species determined after completion of reaction 13 at pH 13 was found to be indentical with that from the reaction of $[FeL_2]^{3+}$ and OH^- as determined spectrophotometrically (Figure 1b). Therefore, it can be concluded that the kinetic titration curve represents the acid–base equilibrium (1), which is established within ≤1 μs at pH > 10. The pK_a value determined by the radiation chemical method is thus the same as that measured by potentiometric or spectrophotometric titration of $[FeL_2]^{3+}$.

The reaction of $[FeL_2]^{2+}$ with $OH^\bullet$ and its conjugate base $O^{\bullet-}$ ($pK_a(OH)$ = 11.8) was studied at pH 12 in N_2O-saturated solutions, which contained 0.02–0.2 mM $[FeL_2]^{2+}$, by observing the buildup of optical density at 542 nm. From the linear dependence of k_{obsd} on $[FeL_2^{2+}]$ the second-order rate constant was found to be 6.4×10^9 M^{-1} s^{-1}. From a comparison of the maximum optical

(41) See: Butler, J.; Land, E. J.; Prütz, F.; Swallow, J. *Biochem. Biophys. Acata* **1982**, *705*, 150 and references therein. For a review, see: Farnier der Violet, P. *Rev. Chem. Intermed.* **1981**, *4*, 121.

Table II. Comparison of a Previous and Present Determination of the Redox Potential of the Couple Ascorbate(1−)/Ascorbate(2−)

pH	$E_{1/2}([FeL_2]^{3+/2+})$,[a] V vs NHE	$E_{1/2}(ASC^{-/2-})$,[b] V vs NHE	$\Delta E_{1/2}$,[c] V	$E_{1/2}(ASC^{-/2-})$,[d] V vs NHE
11	+0.084	+0.052	0.024,[e] 0.052[f]	0.060,[e] 0.032[f]
12	+0.048	+0.022	+0.032	+0.016
13	+0.010	+0.016	−0.010	+0.020

[a] Measured redox potentials (this work, Figure 3). [b] Calculated redox potentials from data in ref 43 (Table IV). [c] Experimental difference of the redox potentials of the couples $[FeL_2]^{3+/2+}$ and $ASC^{-/2-}$ (this work). [d] Experimental redox potentials of the couple $ASC^{-/2-}$ (this work). $E_{1/2}$(exptl) = $E_{1/2}([FeL_2]^{3+/2+}) - \Delta E_{1/2}$. [e] From the approach to equilibrium (see text). [f] From the equilibrium concentration (see text).

density after completion of the reaction with $OH^{\bullet}/O^{\bullet-}$ with that from the reaction with $(SCN)_2^{\bullet-}$, which is assumed to react quantitatively by electron transfer, the yield of electron transfer was found to correspond to 90%. The remaining 10% is assigned to H abstraction from the ligands of $[FeL_2]^{2+}$. These numbers show that the highly reactive $OH^{\bullet}/O^{\bullet-}$ radical exhibits a remarkable preference for oxidizing the metal center.

In order to decrease the reactivity and thereby increase the selectivity of an oxygen-centered radical, a substituent attached to the oxygen may be introduced that is capable of delocalizing the unpaired spin. An example for this is the phenoxyl radical, which has been shown to possess oxidizing properties.[42,43] The phenoxyl radical is rapidly produced by reaction of $OH^{\bullet}/O^{\bullet-}$ with phenolate[44,45] (eq 14). The reaction between $C_6H_5O^{\bullet}$ and

$$OH^{\bullet}/O^{\bullet-} + C_6H_5O^- \xrightarrow{H_2O} C_6H_5O^{\bullet} + 2OH^- \quad (14)$$

$[FeL_2]^{2+}$ was studied by using a solution at pH 13 that contained 10 mM phenol and 0.1–0.5 mM $[FeL_2]^{2+}$ and monitoring the absorption at 398 nm, where $C_6H_5O^{\bullet}$ absorbs,[44,46] and at 542 nm. Under these conditions ≥95% of the $OH^{\bullet}$ radicals react with phenol to give phenoxyl radicals (eq 14). At 398 nm, after the initial rapid increase, a decrease of optical density was observed, whose rate increased with increasing $[FeL_2^{2+}]$. At 542 nm a corresponding increase was observed, demonstrating that $C_6H_5O^{\bullet}$ oxidizes $[FeL_2]^{2+}$ to yield the blue amidoiron(III) species $[FeL(L\text{-}H)]^{2+}$ (eq 15). From the linear dependence of the rates

$$C_6H_5O^{\bullet} + [FeL_2]^{2+} + OH^- \rightarrow C_6H_5O^- + [Fe^{III}L(L\text{-}H)]^{2+} + H_2O \quad (15)$$

measured at 398 and 542 nm the bimolecular rate constant was obtained as 2.4×10^9 M^{-1} s^{-1}. The yield of iron(III) from reaction 15 is the same as that from the reaction with $X_2^{\bullet-}$, i.e. 100%.

A further delocalized radical of the oxyl type is that derived from the dianion ascorbate.[47,48] The question is whether this radical is able to oxidize $[FeL_2]^{2+}$ or whether the parent ascorbate reduces $[Fe^{III}L(L\text{-}H)]^{2+}$. Experiments were performed with 10 mM Br^- solutions at pH 12–13 that contained 0.5–1 mM ascorbate and $[FeL_2]^{2+}$ in concentration ratios that varied between 20:1 and 1:20. Under these conditions the $OH^{\bullet}$ radicals produced by the electron pulse are essentially quantitatively scavenged by the excess Br^- to yield $Br_2^{\bullet-}$. $Br_2^{\bullet-}$ then oxidizes $[FeL_2]^{2+}$ and the ascorbate dianion via reaction 16.[42,47]

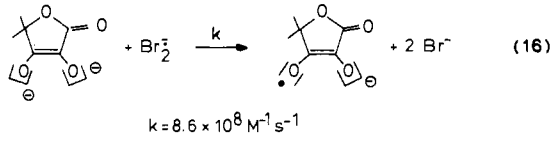

(16)

$k = 8.6 \times 10^8$ M^{-1} s^{-1}

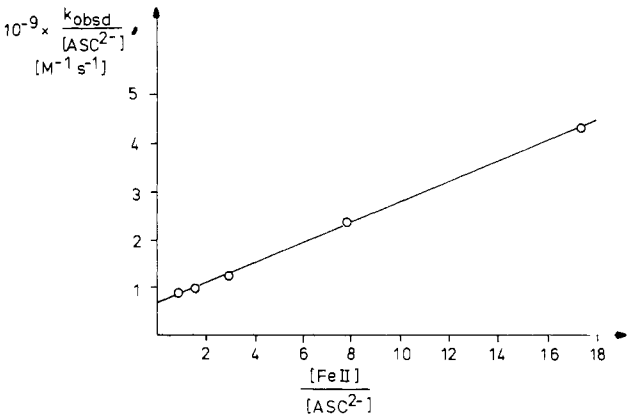

Figure 7. Dependence of $k_{obsd}/[ASC^{2-}]$ vs $[FeL_2^{2+}]/[ASC^{2-}]$ for the determination of k_f (intercept) and k_r (slope) in eq 17 at pH 12.

At concentrations of $[FeL_2]^{2+}$ and ascorbic acid of 0.1 mM, reactions 13 and 16 are complete in ≤20 μs. After this time there are simultaneously present the following species: (i) ascorbate(2−), (ii) the ascorbate(1−) radical, (iii) $[FeL_2]^{2+}$, and (iv) $[FeL(L\text{-}H)]^{2+}$. By monitoring the optical density at 542 nm (where $[FeL(L\text{-}H)]^{2+}$ absorbs) and at 360 nm (where the ascorbate radical absorbs[42]) it was found that $[Fe^{III}L(L\text{-}H)]^{2+}$ oxidizes ascorbate(2−) to give the ascorbate(1−) radical, $ASC^{\bullet-}$. However, this reaction does *not* go to completion but leads to an electron-transfer equilibrium (eq 17). The position of this equilibrium

$$[Fe^{III}L(L\text{-}H)]^{2+} + ASC^{2-} + H_2O \underset{k_r}{\overset{k_f}{\rightleftharpoons}} [FeL_2]^{2+} + ASC^{\bullet-} + OH^- \quad (17)$$

is dependent on pH. The equilibrium constant $K = k_f/k_r$ was determined at two different pH values by using two methods: (a) the rate of approach-to-equilibrium method,[49] which yields k_f and k_r (Figure 7), and (b) measurement of the concentrations at equilibrium of the species involved. The values measured at pH 12 and 13 are K = 3.82 and 0.72, respectively, independent of the experimental method.

By use of the Nernst equation, the equilibrium constants can be converted into differences in redox potentials between the couples $ASC^{\bullet-}/ASC^{2-}$ and $[FeL_2]^{2+}/[Fe^{III}L(L\text{-}H)]^{2+}$. The pH-dependent redox potential for the former couple has been determined previously,[50] and that for the latter has been measured by cyclic voltammetry (see above). The relevant data are summarized in Table II.

Column 2 of Table II contains the redox potentials of the couple $[FeL_2]^{3+/2+}$ at pH 12 and 13 measured by cyclic voltammetry, column 3 shows the corresponding values calculated from the previously published data of the $ASC^{-/2-}$ couple,[43] column 4 contains the differences in redox potentials between the couples $ASC^{-/2-}$ and $[Fe^{III}L(L\text{-}H)]^{2+}/[Fe^{II}L_2]^{2+}$, and column 5 shows the experimental differences in redox potentials between ascorbate and $[FeL(L\text{-}H)]^{2+}$ (Δ(column 2 − column 4)). The agreement between data in column 3 and those in column 5 is good at pH

(42) Schuler, R. H. *Radiat. Res.* **1977**, *69*, 417.
(43) Steenken, S.; Neta, P. *J. Phys. Chem.* **1979**, *83*, 1134.
(44) Land, E. J.; Ebert, M. *Trans. Faraday Soc.* **1967**, *63*, 1181.
(45) Steenken, S. *J. Chem. Soc., Faraday Trans. 1*, in press.
(46) Schuler, R. H.; Buzzard, G. K. *Int. J. Radiat. Phys. Chem.* **1976**, *8*, 563.
(47) (a) Larof, G. P.; Fessenden, R. W.; Schuler, R. H. *J. Am. Chem. Soc.* **1972**, *94*, 9062. (b) Steenken, S.; Olbrich, G. *Photochem. Photobiol.* **1973**, *18*, 43.
(48) Schöneshöfer, M. *Z. Naturforsch., B: Anorg. Chem., Org. Chem., Biochem., Biophys., Biol.* **1972**, *27B*, 649.
(49) (a) Ilan, Y. A.; Czapski, G.; Meisel, D. *Biochem. Biophys. Acta* **1976**, *430*, 209. (b) Wardunan, P.; Clarke, E. D. *J. Chem. Soc., Faraday Trans. 1*, **1976**, *72*, 1377.
(50) Steenken, S.; Neta, P. *J. Phys. Chem.* **1982**, *86*, 3661.

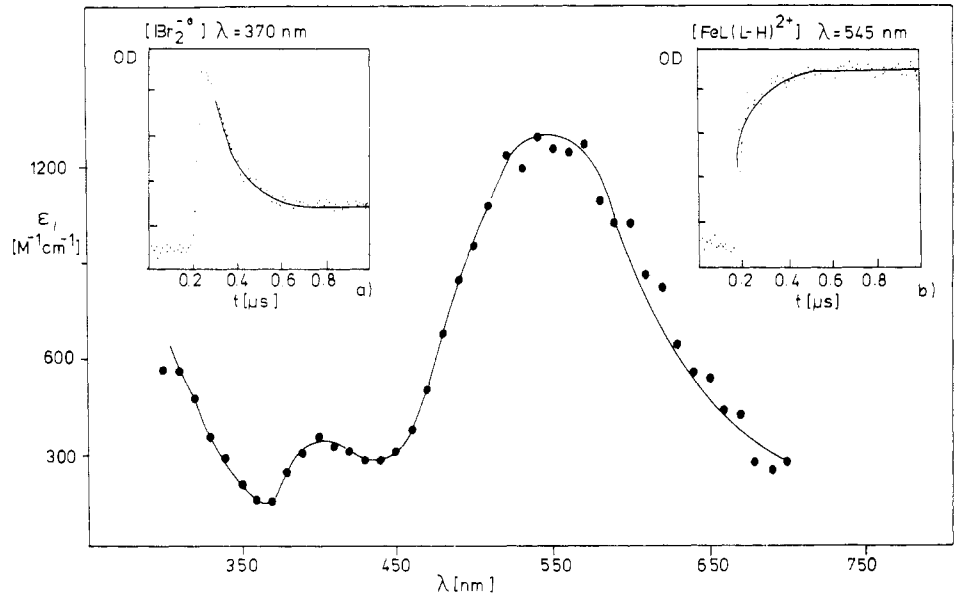

Figure 8. Product spectrum of reaction 18 in the presence of Br^- and of the $e^-(aq)$ scavenger N_2O at pH 12.1. Insets: (a) decrease of the concentration of $Br_2^{\bullet-}$ as a function of time at 370 nm; (b) rate of formation of $[FeL(L\text{-}H)]^{2+}$ at 545 nm ($[Fe] = 1.03 \times 10^{-3}$ M, $[Br^-] = 10^{-2}$ M).

12 and still reasonable at pH 13. This result nicely confirms the previous determination[50] of the redox potential of the couple $ASC^{\bullet-}/ASC^{2-}$.

Laser Photolysis Experiments. Aqueous solutions containing 1 mM $[FeL_2]^{2+}$ at pH 8–13 were photolyzed with 20-ns pulses (pulse energy 20–250 mJ) from a KrF excimer laser (λ = 248 nm), and the changes in optical density resulting from the laser pulse were recorded by using a computer-controlled detection system. At wavelengths above 400 nm a very strong signal was observed. It shows a maximum at ~700 nm, and it is assigned to the hydrated electron, $e^-(aq)$:

$$[FeL_2]^{2+} \xrightarrow[\text{pH 8–10}]{h\nu} [FeL_2]^{3+} + e^-(aq) \qquad (18)$$

The same spectrum was observed on photolysis of 2 mmol KI solutions, which are known to produce $I^\bullet$ and $e^-(aq)$ in a monophotonic process with a quantum yield of 0.29.[51] In agreement with this assignment, the absorption above 400 nm can be removed by the addition to the solution of known $e^-(aq)$ scavengers, e.g. N_2O, O_2, or halocarbons such as CH_2Cl_2. By comparing the $e^-(aq)$ yield from $[FeL_2]^{2+}$ with that from KI, the quantum yield for the photoionization of $[FeL_2]^{2+}$ was determined to be 0.29 at pH 8-10 and 0.36 at pH 12.4. This process is monophotonic, as was concluded from the linear dependence of the $e^-(aq)$ yield on the laser pulse intensity, which was varied by a factor of 10 in the range 10–100 mJ.

The yield of photooxidation of $[FeL_2]^{2+}$ can be increased by converting $e^-(aq)$ into a species that is able to oxidize $[FeL_2]^{2+}$. This was done by using N_2O and Br^-. An example for this reaction at pH 12.1 is shown in Figure 8 and in the insets. Inset a shows the decrease of the concentration of $Br_2^{\bullet-}$, monitored at 370 nm, that results from its reduction by $[FeL_2]^{2+}$; in inset b the formation of the blue amidoiron(III) species at 545 nm, $[Fe^{III}L(L\text{-}H)]^{2+}$, is demonstrated. The rates measured at these two wavelengths are the same, and they are proportional to the concentration of $[FeL_2]^{2+}$. The rate constants for the reaction of $[FeL_2]^{2+}$ with $Br_2^{\bullet-}$ (eq 13), determined from this linear dependence of k_{obsd} on $[FeL_2^{2+}]$, is 6.3×10^9 M^{-1} s^{-1}, equal to that measured for the same reaction by radiolysis (see above).

Since photoionization provides a particularly simple way of quantitative production of $[FeL_2]^{3+}$ (pH 8–11) and of its deprotonated form (pH >11), this method was used to determine its pK_a value to be 11.6 in excellent agreement with the previous determinations.

Since the radicals $I_2^{\bullet-}$ and $(SCN)_2^{\bullet-}$ may also be produced photochemically, we have checked the results obtained by pulse radiolysis for the oxidation of $[FeL_2]^{2+}$ by these radicals by means of laser photolysis experiments. A deoxygenated 2 mM solution of potassium iodide (absorbance at 248 nm = 1.3 cm^{-1}) was photolyzed, and the production of $I_2^{\bullet-}$ and $e^-(aq)$ was observed (eq 19 and 20). On addition of N_2O $e^-(aq)$ disappeared and it

$$I^- \xrightarrow{h\nu} I^\bullet + e^-(aq) \qquad (19)$$

$$I^\bullet + I^- \rightarrow I_2^{\bullet-} \qquad (20)$$

was replaced by an equivalent amount of $I_2^{\bullet-}$. On addition of 0.1–1.0 mM $[FeL_2]^{2+}$ at pH 12.1 $I_2^{\bullet-}$ rapidly disappeared (monitored at 390 nm) and $[Fe^{III}L(L\text{-}H)]^{2+}$ was formed (monitored at 542 nm) at the same rate. From the linear dependencies of the rates of decay of $I_2^{\bullet-}$ or of production of $[Fe^{III}L(L\text{-}H)]^{2+}$ on $[FeL_2^{2+}]$ a second-rate constant of 8.8×10^9 M^{-1} s^{-1} was calculated, which is equal with the value from pulse radiolysis measurements. Analogous experiments were performed with 20 mM SCN^- solutions. The bimolecular rate constant for the reaction between $[FeL_2]^{2+}$ and $(SCN)_2^{\bullet-}$ of 7.7×10^9 M^{-1} s^{-1} agrees again excellently with the value determined from pulse radiolysis.

Summary

We have shown that the orange low-spin bis(1,4,7-triazacyclononane)iron(III) trication is reversibly deprotonated (one proton per Fe(III)) in alkaline aqueous solution (pK_a = 11.6 ± 0.4) forming a blue species. The electronic ground state of this intermediate must be described as low-spin amidoiron(III) species. The aminylradical iron(II) formulation describes an electronically excited state produced via ligand-to-metal charge transfer.

Under anaerobic conditions the blue intermediate disproportionates slowly, forming $[FeL_2]^{2+}$ (50%), $[Fe^{II}L(OH)_2)_3]^{2+}$, and an unidentified two-electron-oxidation product of the cyclic triamine. In the presence of an external oxidant (O_2, H_2O_2) the products are $[LFe(OH_2)_3]^{3+}$ and one oxidized ligand.

Amidoiron(III) intermediates are the primary reactive species in the oxidative dehydrogenation reaction of primary or secondary

(51) Jortner, J.; Ottolenghi, M.; Stein, G. *J. Phys. Chem.* **1962**, *66*, 2029, 2037, 2042; **1964**, *68*, 247.

(52) This proposed mechanism involves an aminyl radical–iron(III) (or an amidoiron(IV)) intermediate that has not been experimentally identified. An alternative path involving disproportionation of two aminyl radical–iron(II) species is also conceivable. Both mechanisms lead to the formation of a very strained iminoiron(II) product (50%), which could undergo rapid carbinolamine formation in the presence of the relatively high $[OH^-]$ used, thereby relieving the strain. (We thank a reviewer for pointing this out to us.)

amines in (amine)iron(III) complexes, yielding imine- or di-imine-iron(II) complexes.

The oxidation of $[FeL_2]^{2+}$ with a variety of pulse radiolytically generated radicals produced $[FeL_2]^{3+}$, and at pH >10 the $[FeL(L\text{-}H)]^{2+}$ species at nearly diffusion controlled rates. Laser photolysis (λ = 248 nm) of $[FeL_2]^{2+}$ at pH 8-13 produced in a monophotonic process the hydrated electron and $[FeL_2]^{3+}$ (or its deprotonated form).

Finally it was shown that $[FeL(L\text{-}H)]^{2+}$ reduces the ascorbate dianion, yielding $[FeL_2]^{2+}$ and the ascorbate radical anion. From equilibrium kinetics of this reaction it has been possible to confirm a previous determination of the redox potential of the $AS^{-/2-}$ couple.

Acknowledgment. We are grateful to the Fonds der Chemischen Industrie for financial support of this work.

Registry No. $[FeL_2](ClO_4)_2$, 111958-64-6; $[FeL_2](ClO_4)_3$, 111958-66-8; $[FeL(L\text{-}H)]^{2+}$, 111958-67-9; $I_2^{\bullet-}$, 12190-71-5; $(SCN)_2^{\bullet-}$, 34504-17-1; $Br_2^{\bullet-}$, 12595-70-9; $OH^{\bullet}$, 3352-57-6; $PhO^{\bullet}$, 2122-46-5; H_2O_2, 7722-84-1; O_2, 7782-44-7; ascorbate(1-), 299-36-5; ascorbate(2-), 63983-50-6; 1,4,7-triazacyclononane, 4730-54-5.

Contribution from the Department of Chemistry, Faculty of Science, Kyushu University 33, Hakozaki, Fukuoka, 812 Japan, and Coordination Chemistry Laboratories, Institute for Molecular Science, Myodaiji, Okazaki, 444 Japan

An Important Factor Determining the Significant Difference in Antiferromagnetic Interactions between Two Homologous (μ-Alkoxo)(μ-pyrazolato-N,N')dicopper(II) Complexes[1]

Yuzo Nishida[2a] and Sigeo Kida*[2b]

Received February 2, 1987

The crystal structures of $Cu_2(L^1)(prz)$ (**1**) and $Cu_2(L^2)(pyz)$ (**2**) were determined by X-ray analysis, where prz denotes a deprotonated anion of pyrazole and HL^1 and HL^2 represent binucleating ligands formed by the condensation of salicylaldehyde with 1,3-diamino-2-propanol and 1,5-diamino-3-pentanol, respectively. Both compounds consist of discrete binuclear units, in which copper atoms are linked by the alkoxide oxygen of the ligand and the pyrazolate nitrogens. Magnetic susceptibility measurements revealed that antiferromagnetic interaction is operating in both compounds. However, the interaction of **2** ($-2J$ = 595 cm^{-1}) is much stronger than that of **1** ($-2J$ = 310 cm^{-1}), irrespective of the small difference in the bridging structure. It is difficult to explain this fact in terms of structural factors on the basis of the so far widely accepted criterions. Instead, the change in the interaction between the magnetic d orbitals and the HOMOs of the pyrazolate nitrogens induced by changes in the size of the chelating rings was estimated for the energy and overlap of these orbitals. It was concluded that the pyrazolate bridge contributes little to the antiferromagnetism of **2**, but in the case of **1**, the pyrazolate bridge operates countercomplementarily toward the antiferromagnetism effected by the alkoxide bridge, bringing about the weaker antiferromagnetism for **1**.

Introduction

Magnetisms of bis(μ-hydroxo)- or bis(μ-alkoxo)dicopper(II) complexes have been the subjects of extensive investigations for the last two decades.[3] According to Hatfield and Hodgson, antiferromagnetic interaction between copper(II) ions becomes larger with increasing Cu-O-Cu angle in these complexes.[3,4] This was reasonably explained in terms of quantum-mechanical treatments by Hoffmann et al.,[5] Bencini and Gatteschi,[6] Kahn,[7] and Astheimer and Haase.[8] However, this rule had been confined to doubly bridged systems with the Cu-O-Cu angle in the range 95-105° until McKee et al.[9] and the present authors[10] reported the syntheses and magnetism of copper(II) complexes with a single alkoxide bridge derived from 1,3-diamino-2-propanol, such as **3** (Figure 1). Since in such complexes the Cu-O-Cu angle is much larger (120-135°) than that of the doubly bridged complexes, substantially stronger antiferromagnetic interaction would be expected in spite of the fact that the superexchange paths occur through half of the doubly bridged complexes. In fact, this was found to be true; e.g., $2J = -635$ cm^{-1} for **3**.[10] It was revealed that when another bridging group, such as acetate[10] or azide (end to end),[11] is added to this system, the antiferromagnetic interaction is substantially weakened or enhanced, depending on the second ligand. This fact was reasonably interpreted in terms of Hoffmann's theory that the matching of symmetries of HOMOs of the bridging groups determines whether the two bridges work complementarily or countercomplementarily in the superexchange interaction.[10] This theory is essentially important when the magnetism of a binuclear complex possessing two different bridging groups is considered. This fact has been recognized in some other examples.[11,12]

Recently, Mazurek et al. reported the preparation of dicopper(II) complexes $Cu_2(L^1)(prz)\cdot H_2O$ (**1**·H_2O) and $Cu_2(L^2)(prz)$ (**2**), where H_3L^1 and H_3L^2 are Schiff bases derived from salicylaldehyde and 1,3-diamino-2-propanol or 1,5-diamino-3-pentanol (Figure 2).[13] They determined the crystal structure of

(1) Partly presented at the 25th International Symposium on Coordination Chemistry in Nangjing, China, Aug 1987; see Abstracts, p 105.
(2) (a) Kyushu University. Present address: Department of Chemistry, Faculty of Science, Yamagata University, Koshirakawamachi, Yamagata, 990 Japan. (b) Institute for Molecular Science.
(3) Crawford, U. H.; Richardson, H. W.; Wasson, J. R.; Hodgson, D. J.; Hatfield, W. E. *Inorg. Chem.* **1976**, *15*, 2107.
(4) (a) Hatfield, W. E. *ACS Symp. Ser.* **1974**, *No. 5*, 108. (b) Hodgson, D. J. *Prog. Inorg. Chem.* **1975**, *19*, 173.
(5) Hay, P. J.; Thibeault, J. C.; Hoffmann, R. *J. Am. Chem. Soc.* **1975**, *97*, 4887.
(6) Bencini, A.; Gatteschi, D. *Inorg. Chim. Acta* **1978**, *31*, 11.
(7) Kahn, O. *Inorg. Chim. Acta* **1982**, *62*, 3.
(8) Astheimer, H.; Haase, W. *J. Chem. Phys.* **1986**, *85*, 1427.
(9) (a) McKee, V.; Smith, J. *J. Chem. Soc., Chem. Commun.* **1983**, 1465. (b) Drew, M. G. B.; Nelson, J.; Esho, F. S.; McKee, V.; Nelson, S. M. *J. Chem. Soc., Dalton Trans.* **1982**, 1837.
(10) (a) Nishida, Y.; Takeuchi, M.; Takahashi, K.; Kida, S. *Chem. Lett.* **1985**, 631. (b) Nishida, Y.; Kida, S. *J. Chem. Soc., Dalton Trans.* **1986**, 2633.
(11) (a) McKee, V.; Zvagulis, M.; Reed, C. A. *Inorg. Chem.* **1985**, *24*, 2914. (b) McKee, V.; Dagdigian, J. V.; Bau, R.; Reed, C. A. *J. Am. Chem. Soc.* **1981**, *103*, 7000.
(12) Mallah, T.; Baillot, M.-L.; Kahn, O.; Gouteron, J.; Jeannin, S.; Jeannin, Y. *Inorg. Chem.* **1986**, *25*, 3058.

0020-1669/88/1327-0447$01.50/0